Naval Research Laboratory
Washington, DC 20375-5320

NRL/MR/6720--99-8328

Optical Emission Studies of the NRL Plasma Torch for the Shipboard Waste Treatment Program

J. L. GIULIANI
J. ROGERSON
R. W. CLARK
P. KEPPLE
P. PULSIFER

Radiation Hydrodynamics Branch
Plasma Physics Division

D. A. COUNTS
S. H. PETERSON

Geo-Centers, Inc.
Fort Washington, MD

J. W. FLEMING
V. A. SHAMAMIAN
B. D. SARTWELL

Surface Chemistry Branch
Chemistry Division

February 26, 1999

REPORT DOCUMENTATION PAGE

Form Approved
OMB No. 0704-0188

1. AGENCY USE ONLY (*Leave Blank*)	2. REPORT DATE	3. REPORT TYPE AND DATES COVERED
	February 26, 1999	

4. TITLE AND SUBTITLE

Optical Emission Studies of the NRL Plasma Torch for the Shipboard Waste Treatment Program

5. FUNDING NUMBERS

6. AUTHOR(S)

J.L. Giuliani, D.A. Counts,* J. Rogerson, R.W. Clark, P. Kepple, P. Pulsifer, J.W. Fleming, V.A. Shamamian, S.H. Peterson,* and B.D. Sartwell

7. PERFORMING ORGANIZATION NAME(S) AND ADDRESS(ES)

Naval Research Laboratory
Washington, DC 20375-5320

8. PERFORMING ORGANIZATION REPORT NUMBER

NRL/MR/6720--99-8328

9. SPONSORING/MONITORING AGENCY NAME(S) AND ADDRESS(ES)

Office of Naval Research, 800 N. Quincy Street, Arlington, VA 22217-5660
Naval Surface Weapons Center, Carderock Division, Bethesda, MD 20084

10. SPONSORING/MONITORING AGENCY REPORT NUMBER

11. SUPPLEMENTARY NOTES

*Geo-Centers, Inc., Fort Washington, MD

12a. DISTRIBUTION/AVAILABILITY STATEMENT

Approved for public release; distribution unlimited.

12b. DISTRIBUTION CODE

A

13. ABSTRACT (*Maximum 200 words*)

Optical emission spectroscopy is employed to characterize the plasma in the NRL torch operating at ~100 kW DC power. Both non-transferred and transferred arc configurations are considered. The working gas of the torch is nitrogen with a 5% admixture of hydrogen. Atomic emission lines are measured and analyzed using a local thermodynamic equilibrium (LTE) and a collisional radiative equilibrium (CRE) model. The core of the arc is found to be close to LTE, with a central plasma temperature of 6,200°K in the non-transferred mode, and ~15,000°K in the transferred mode. However, the periphery of the arc is far from thermal and excitation equilibrium. Radiative photo-pumping by the hot core, included in the CRE model, is found to play a significant role in controlling excited level populations. Stark broadened H_β measurements of the non-transferred arc indicate an anamolously high electron density. For the transferred arc the plasma radiation accounts for ~50% of the energy input to the plasma. Finally, the electrical properties of long transferred arcs are found to change during slag processing due to entrainment of volatized slag material with low ionization potential. This suggests an on-line diagnostic for the process state of the treated waste.

14. SUBJECT TERMS

Plasma torches
Plasma diagnostics
Transferred and non-transferred arcs
Optical emission spectroscopy
Shipboard waste treatment

15. NUMBER OF PAGES

30

16. PRICE CODE

17. SECURITY CLASSIFICATION OF REPORT	18. SECURITY CLASSIFICATION OF THIS PAGE	19. SECURITY CLASSIFICATION OF ABSTRACT	20. LIMITATION OF ABSTRACT
UNCLASSIFIED	UNCLASSIFIED	UNCLASSIFIED	UL

Contents

OPTICAL EMISSION LINE STUDIES OF THE NRL PLASMA TORCH FOR THE SHIPBOARD WASTE TREATMENT PROGRAM

I. Introduction

Plasma arcs have long been used in materials processing applications. Examples include production of acetylene [1], heating of steel in a tundish [2], and plasma spray coatings [3]. The application of plasma arc technology to materials waste processing has evolved over the past decade. Retech's Plasma Arc Centrifugal Treatment (PACT) design was first tested with a transferred arc using a bench-size unit in 1987. Today, operating waste treatment systems run at the hundred kilowatt to several megawatt power level, with waste crucibles up to eight feet in diameter in the largest systems.

Although the arc technology is well in hand, the successful application of torches in novel systems requires testing, evaluation, and understanding of potential designs. This is indicated by the recent development of a number of simulation models for efficiency and design scaling of high current devices [4,5,6,7]. In the Plasma Arc Waste Destruction System (PAWDS) for shipboard waste treatment one has a unique design tradeoff between efficiency and size, the latter quantity being of little concern in land based systems but of primary concern on board seafaring vessels. An essential engineering component in the tradeoff issue is the power balance of the system. For a given electrical power input to the plasma how much is transferred to to the anode, to the cathode, to chamber walls by radiation, to the crucible of slag by conduction and ohmic heating, to the ambient gas in the chamber by mixing with the arc gas, and finally how much is carried off by the exhausting gases. Experimental investigations on the power balance have been performed on several high current torch systems [8,9]. Parisi and Gauvin [9] found that heat transfer by radiation is the main mechanism of energy transfer to a surrounding enclosure for a long transferred arc of argon or nitrogen. Since the radiated power is a strong function of

Manuscript approved December 21, 1999.

the arc gas temperature (proportional to the fourth power of temperature if the plasma were a blackbody emitter), an essential parameter characterizing a plasma arc is its temperature. If local thermodynamic equilibrium (LTE) is assumed, then a knowledge of the input gas constituents, chamber pressure p, and measured arc gas temperature T_g is sufficient to determine the plasma conditions. In particular, the composition of the heated gas, including the electron density n_e is specified by T_g and p.

This report discusses the use of optical emission spectroscopy (OES) to characterize the plasma in both the non-transferred and transferred arc configuration of the NRL torch system. The temperature measurement is a starting point for the analysis of the power balance relation in the system. First, spatially resolved, broadband optical measurements of emission lines from atomic hydrogen in the plasma are used to estimate the electron temperature [$T_e(r)$] profile across the arc. The arc plasma is assumed to be radially symmetric and r is the radial coordinate within the arc. The analyzed results indicate that the core of the arc is close to LTE with a central temperature of 6,200°K in the non-transferred mode and ~15,000°K in the transferred mode. However, in the outer periphery of the arc, called the mantle, conditions are far from equilibrium. Photo-absorption of the radiation emitted from the core plays a significant role in determining the internal energy of the gas in the mantle. A second program was begun to measure n_e through Stark broadening, This information can also be used to investigate the equilibrium condition. Limited spectral data suggest that n_e is ~800 times larger than one would expect from the LTE assumption ($n_e \simeq 10^{14}$ cm^{-3}) using the above temperature at atmospheric pressure. The conclusion of non-equilibrium conditions would appear to be quite unusual given the classic work of Maecker [10,11]. We note, however, that other recent observations also indicate a significant departure from LTE [12] in arcs. A third program in OES consisted of broadband surveys taken during treatment of standard waste slags with a transferred arc. The spectra demonstrated a clear entrainment process of the vapor from heated waste slag into the core of the arc which affects the conductivity of the plasma.

II. OES Analysis of the Non-Transferred Arc

The spectroscopic setup for the NRL torch system is depicted in Fig. 1. During the observations the torch is kept is the vertical position and translated along the z-axis which intercepts the center of the crucible. Emission from the arc passes through a narrow collimator port at the rear of the chamber which is sealed with a sapphire window. A pinhole behind the window and lens system combine to form an image of the arc with parallel rays subject to a factor of four de-magnification. An optical fiber matched to the lens system and mounted on a translatable stage detects the image. The visible emission from the arc is about a centimeter in diameter and the fiber is stepped so that a spectrum is acquired every 0.2 cm in the y-direction across the arc. The spatial resolution is $\sim$0.1 cm at the position of the arc. Three centimeters of the arc along the vertical z-direction are accessible at the fiber optic plane. Two gratings can be used in the spectrometer, but only results from the low resolution (300 lines/mm) covering the entire optical domain will be discussed here. Each spectra is corrected for the wavelength dependent response function of the optical system.

A sample spectrum is presented in Fig.2. The operating conditions are 333 Volts, 375 Amps, 125 kW, 100 slpm (standard liters per minute) of N_2, with a H_2 seeding of 5 slpm. The system is in the non-transferred mode and the spectra is taken at the center of the arc ($y = 0$), 1 cm down from the torch nozzle. Several prominent atomic emission complexes from neutral nitrogen are noted. Each feature is a combination of three to five individual lines decaying to the ^{4}P term level. The spectral resolution is insufficient to resolve the individual lines. These features will be denoted as N1, N2, and N3. An energy level diagram for neutral nitrogen is shown in Fig.3(a) where the three lines comprising the N1 complex are called out. Molecular emission from N_2 is negligible or at most weak throughout the visible arc. The hydrogen emission lines H_α and H_β are also noted in Fig.2 and the corresponding hydrogen energy level diagram is given in Fig.3(b). These hydrogen features are individual lines and can be used to estimate the electron temperature T_e in the arc. The closer the emission line ratio H_α/H_β is to unity, the higher T_e is.

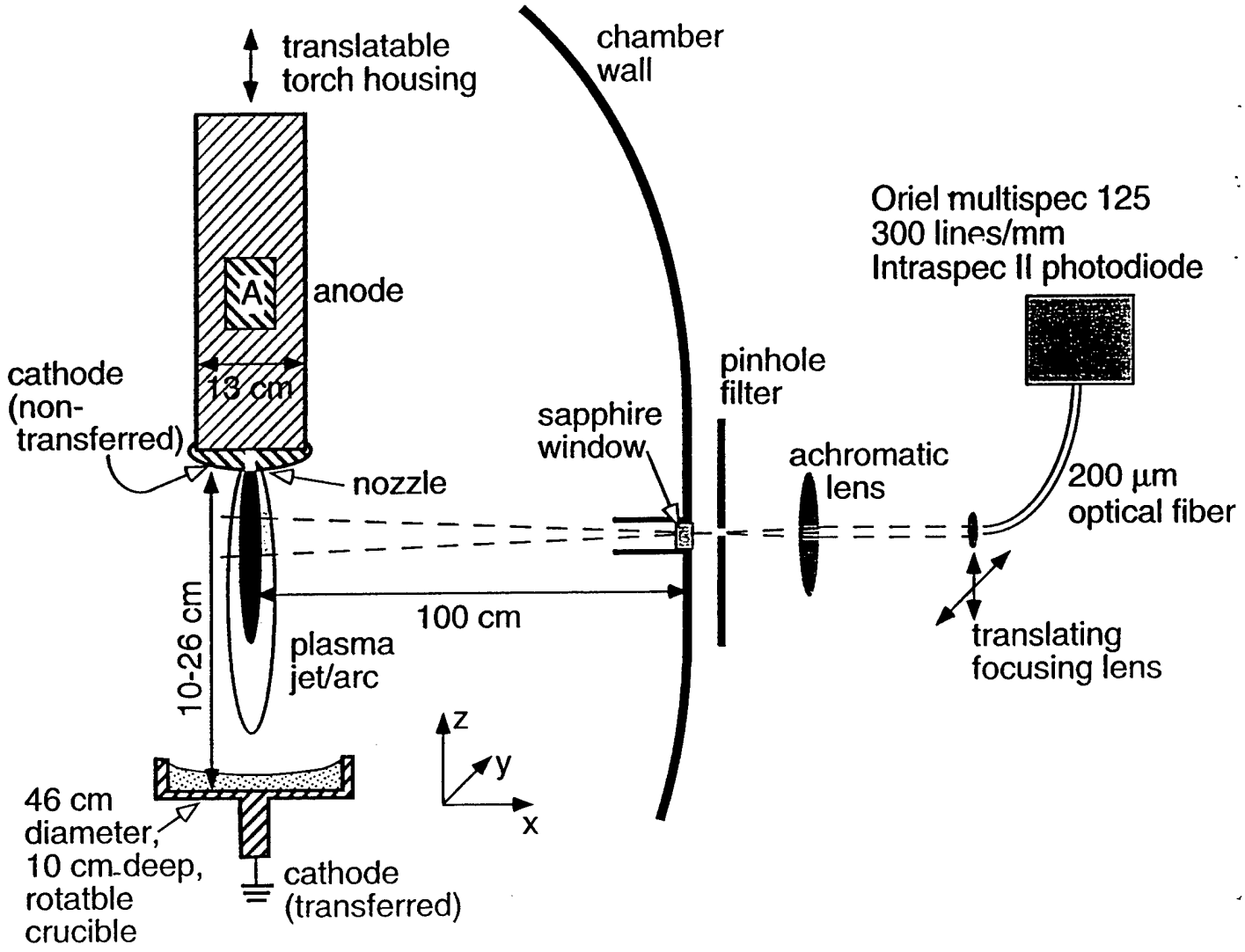

Fig.1 Schematic drawing of the NRL torch chamber and spectroscopic arrangement. The coordinate origin is located at the bottom center of the crucible.

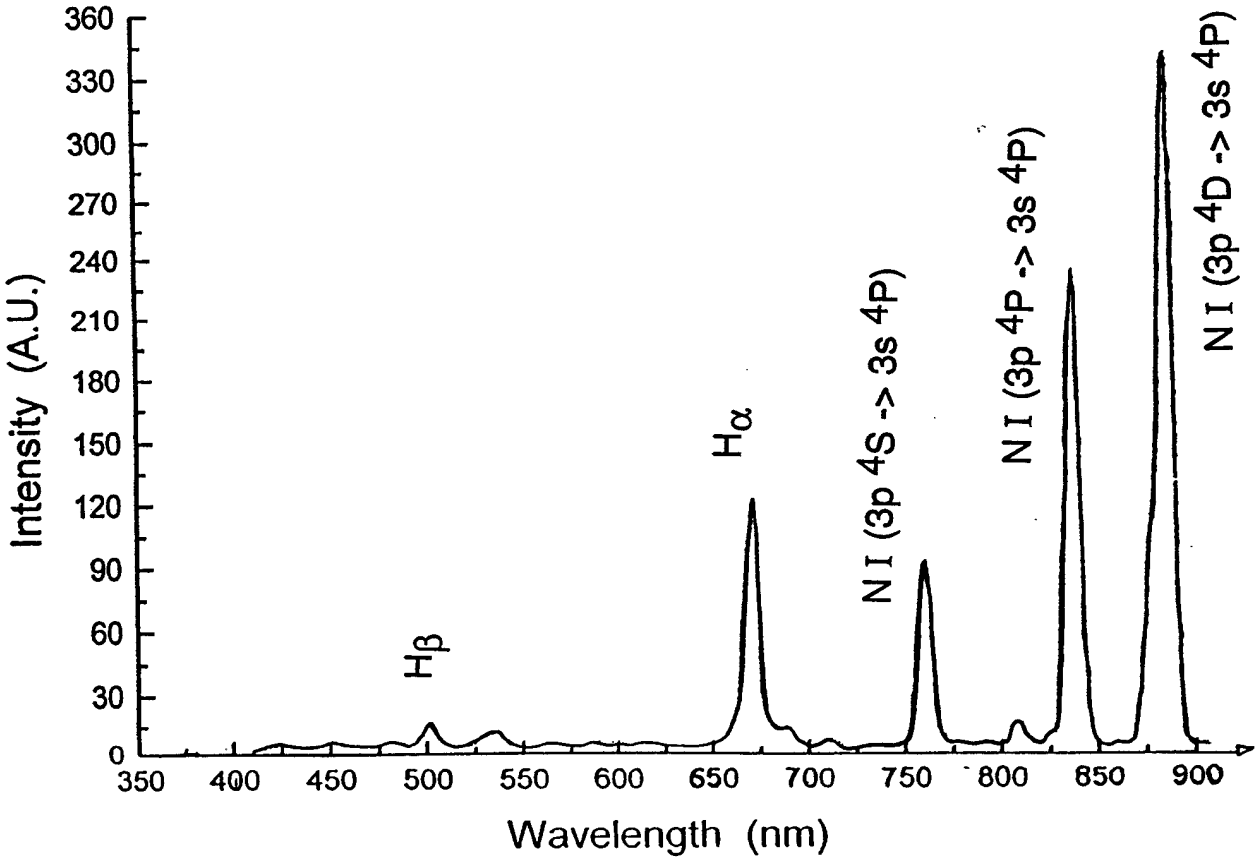

Fig.2 Sample optical spectrum of the plasma arc in the non-tranferred mode taken at the center of the arc ($y = 0$), 1 cm down from the torch nozzle. Emission complexes from neutral nitrogen and lines from neutral hydrogen are noted. The operating conditions are 333 Volts, 375 Amps, 125 kW, 100 slpm (standard liters per minute) of N_2, with a H_2 seeding of 5 slpm.

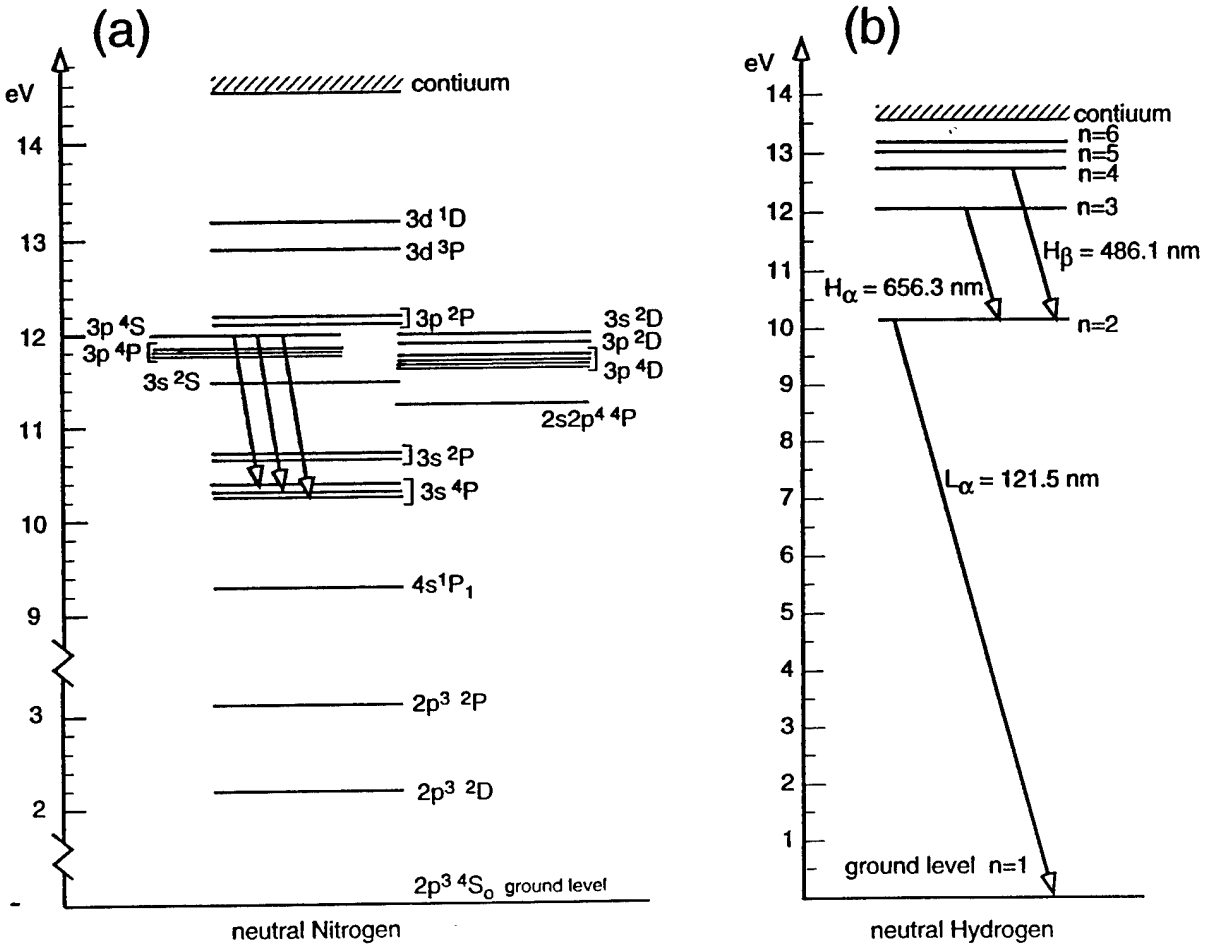

Fig.3 Energy level diagrams for neutral nitrogen (a) and hydrogen (b). 1 eV corresponds to 11,650 °K or 1,240 nm.

Spectra were taken at 15 positions across the arc in the y-direction and at 1, 2, and 4 cm down from the torch nozzle in z, all at the same operating conditions mentioned above. The procedure was duplicated to get a second set of data. Emission line intensities are measured from the spectra after subtracting the continuum background and the ratios H_α/H_β, N1/N2, and N3/N2 are formed. All the data sets are combined to enhance the signal-to-noise ratio. The resulting observed emission ratios are presented in Fig.4(a) for nitrogen and Fig.4(b) for hydrogen. Note that the nitrogen ratios show little dependence on the y-position, while the H_α/H_β ratio displays a dip in the center of the arc, corresponding to a high temperature, and a leveling off in the mantle of the arc.

The data is analyzed according to the following procedure. A Gaussian temperature profile $T_g(r)$ for the gas is assumed in the arc, peaking at the center and decaying to the periphery. The ambient gas temperature in the chamber is measured with thermocouples to be ~1,600°K. For a fixed pressure of 1 atmosphere, an equilibrium calculation is performed for an N_2-H_2 mixture corresponding to the input flow conditions. An example temperature profile and composition calculation is shown in Fig.5. Using the results for atomic nitrogen and hydrogen, two different models for the excited state populations are employed. For the first model, the excited states are assumed to be in LTE with the ionization and Boltzmann statistics readily provide the populations of the excited states. The second model employs collisional radiative equilibrium (CRE) to calculate excited state populations [13,14,15]. The levels included for the population dynamics of nitrogen and hydrogen are those shown in Fig.3 as well as 19 levels N^+ and ionized hydrogen. The processes included in the CRE model are shown schematically in Fig.6(a). They include electron collisional excitation and de-excitation, photo-absorption and radiative decay, electron collisional ionization and three-body recombination, photo-ionization and radiative recombination. If the photo-processes are neglected, the collisional rates reproduce LTE conditions because the rates are detailed balanced. The arc plasma is modeled with twenty radial zones to evaluate the populations. It should be noted that the photo-excitation processes can be non-local, i.e., the self-consistent radiation transfer calculation is coupled to the level rate equations such that emission in one zone

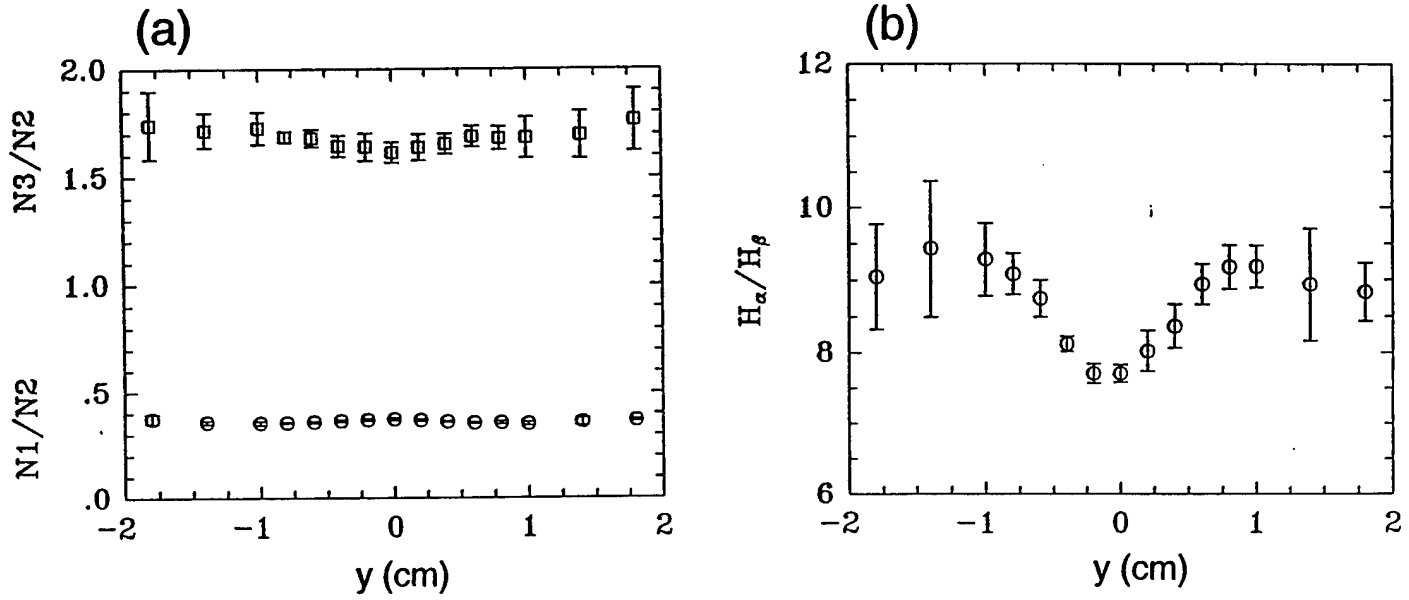

Fig.4 Observed ratios of emission features from nitrogen (a) and hydrogen (b) as a function of y-position across the arc. The error bars denote one sigma standard deviations of six measurements at each position.

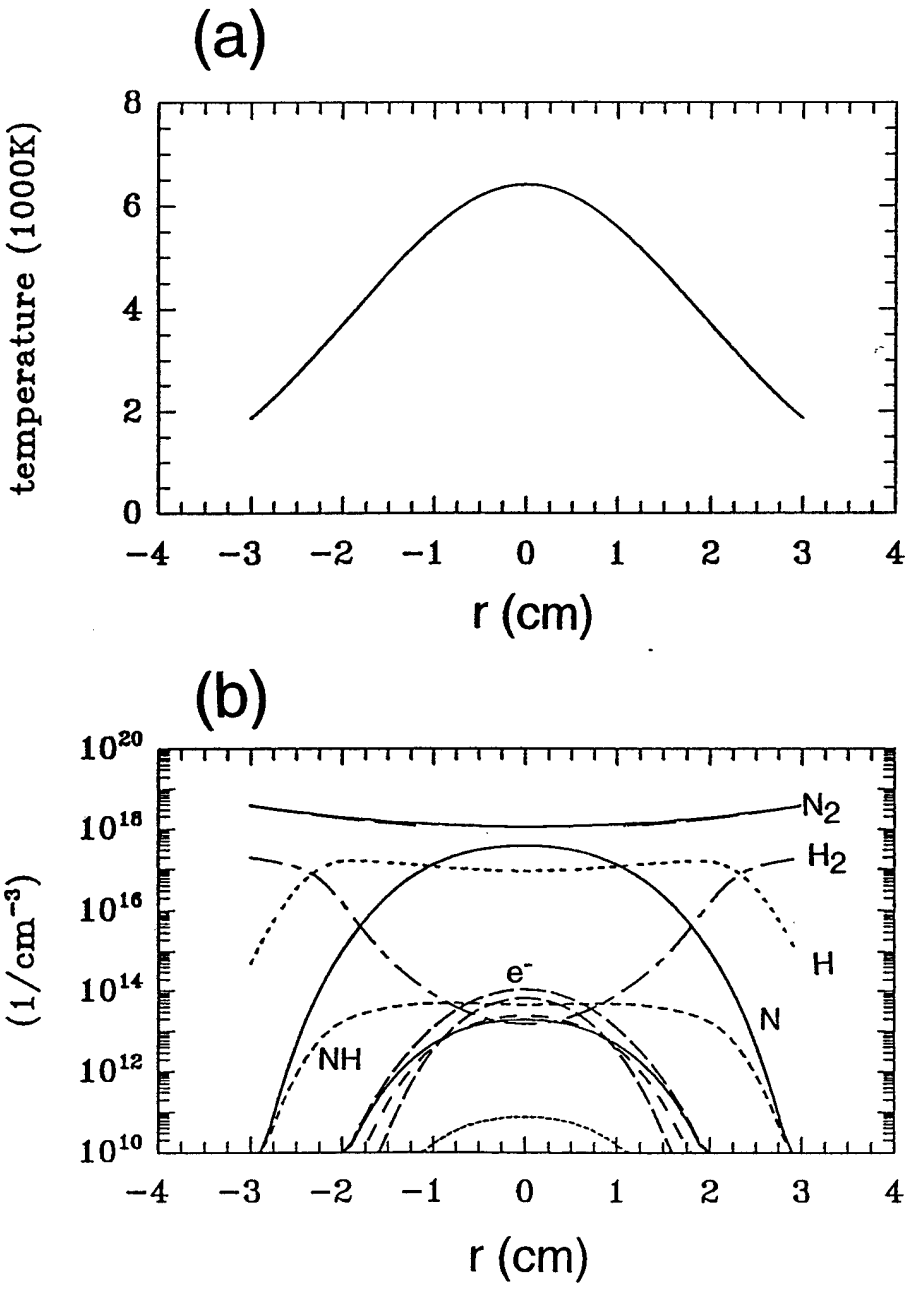

Fig.5 An assumed temperature profile (a) and the corresponding equilibrium densities of the dominant species (b) at one atmosphere along a diameter of the model arc. r is the radial coordinate centered on the arc.

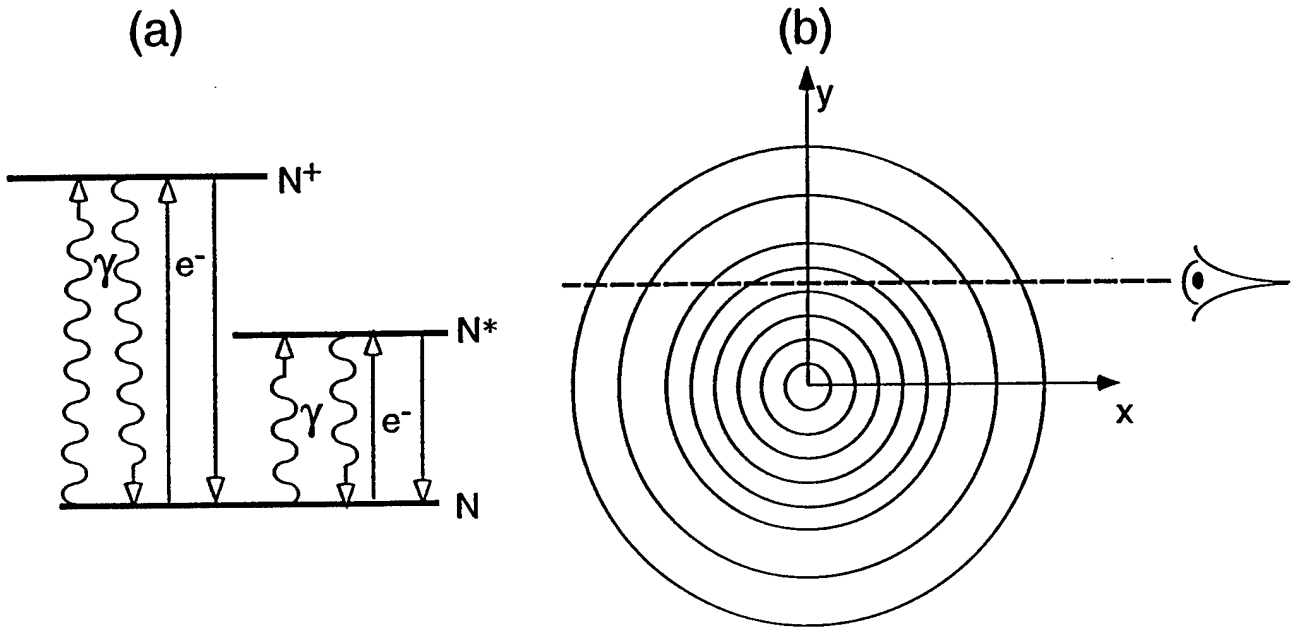

Fig.6 (a) A schematic of the atomic processes included in the collisional radiative equilibrium model to calculate the excited level populations of the atomic species giving rise to the emission lines. (b) The geometry used to calculate the synthetic spectra from the model arc to compare with the observations. The circles represent zones used to numerically calculate the level populations and radiation transport. The impact parameter for calculating the synthetic spectra is measured along the y-direction.

can propagate and subsequently be absorbed in another zone. Based on the population results at different radii from either the LTE case or the CRE case, a post-process, radiative transfer calculation along a line in the x-direction at 15 impact parameters spread in the y-direction is performed to produce the synthetic spectra. A schematic of the transport geometry used to produce the synthetic spectra is shown in Fig.6(b).

Let us begin with the LTE case and consider the ratios for the nitrogen features. In LTE ratios of emission line intensities are a function of T_g alone and the predicted N1/N2 and N3/N2 ratios are shown as the solid lines in Fig.7. As noted above, the observed ratios from Fig.4(a) are weakly dependent upon the y impact parameter and hence only the average value for each ratio is marked at the right side of Fig.7. The observed N3/N2 ratio indicates a high arc temperature ($T_g > 10,000$ °K), while the N1/N2 ratio indicates the opposite ($T_g \sim 2000$ °K). This is the first indication that a simple LTE model for the high powered arc at NRL is not fully consistent with the data.

Next consider the H_α/H_β data and the model calculations. Fig.8 displays the hydrogen data from Fig.4 along with the best fit results from the LTE and CRE models. The temperature profile adopted for this best fit is determined by matching the synthetic spectra to the core of the arc ($y \sim 0$) with the excited state populations determined by the LTE condition. The profile $T_g(r)$ is the one shown in Fig.5. The H_α/H_β ratio in LTE decreases at high temperatures because the populations of the $n = 3$ and $n = 4$ states of hydrogen become nearly equal, while the ratio increases at low temperatures due the predominant population of H($n = 3$) over that of H($n = 4$). The same temperature profile is then used in the CRE model to calculate excited state populations and synthetic spectra. Both the LTE and CRE models are consistent with an equilibrium plasma in the core of the arc at a temperature of 6,200°K. However, in the mantle of the arc, beyond $| y | > 0.8$ cm, the two models diverge dramatically from each other, as well as from the data. In the LTE case, the predicted H_α/H_β ratio continues to rise in the arc periphery due to the decreasing $T_g(r)$. In the CRE case, the turnover in the ratio reflects a photo-absorption effect. The L_α ($n = 1 \rightarrow 2$),

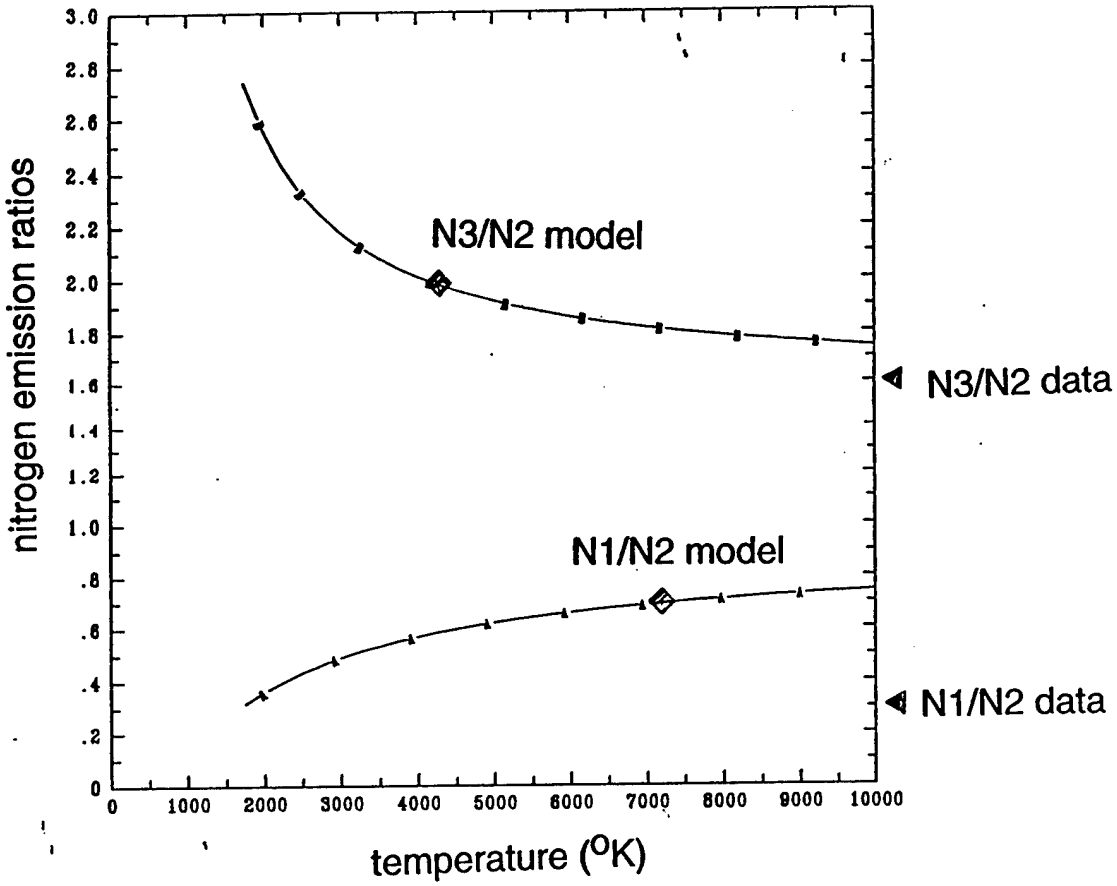

Fig.7 The solid lines are the calculated ratios for the N1/N2 and N3/N2 emission features of nitrogen assuming LTE conditions. The data from Fig.4 are marked on the right side. The model ratios arise from the CRE calculation described in the text.

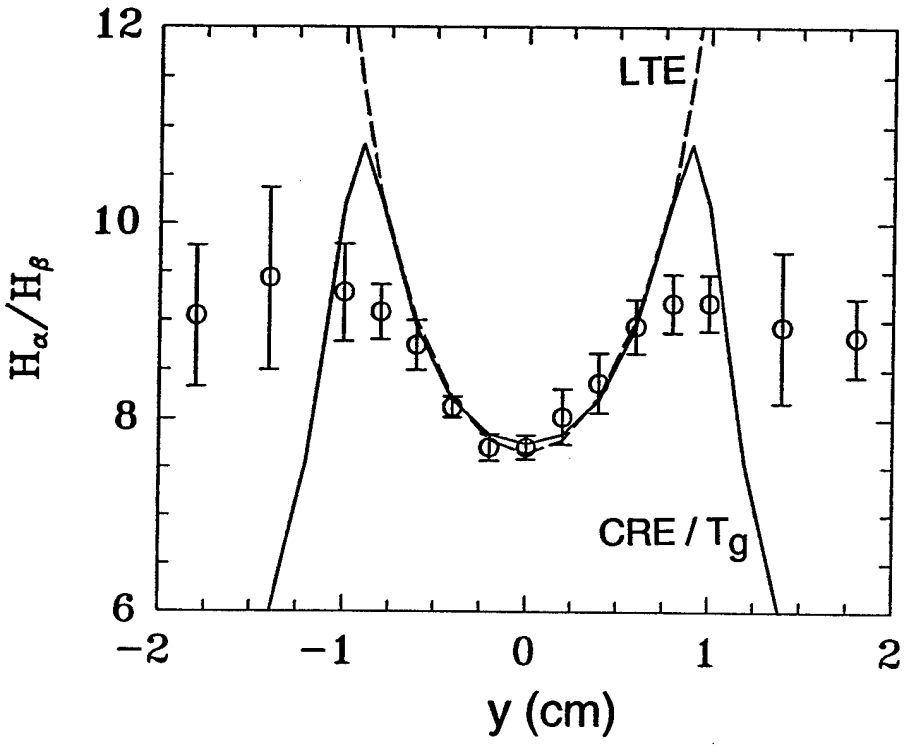

Fig.8 The H_α/H_β emission ratio as predicted from synthetic spectra using the LTE and CRE conditions to determine the excited state populations. The CRE model is a single temperature model. Both models predict a core temperature for the non-transferred arc of 6,200°K, but the results in the arc mantle differ significantly from the data of Fig.4.

L_β ($n = 1 \rightarrow 3$), and L_γ ($n = 1 \rightarrow 4$) photons emitted from the hot core of the arc are absorbed in the cooler mantle and enhance the excited state populations of $n = 2, 3$ and 4 over what they are in LTE. The first Lyman photon (L_α) is depicted in Fig.3(b). Furthermore, in the mantle the mean free path of a L_α photon is smaller than that of a L_β photon, which in turn is smaller than that of a L_γ photon. As a consequence the spectrum hardens, i.e., the low energy photons are removed leaving a more energetic spectrum. At the photon flux propagates into the periphery of the arc the $H(n = 4)$ population becomes anomalously high compared to $H(n = 3)$. This leads to a decrease in the H_α emission compared to that of H_β. To verify that the effect is caused by the inclusion of photo-processes in the CRE model, such processes were turned off in the CRE calculation and the resulting curve for the H_α/H_β ratio followed that found for the LTE case.

The fact that the data matches neither the LTE nor the CRE in the mantle of the arc suggests that the temperature profile in the periphery needs to be revised. One solution found to reproduce the data consists of a two temperature model. The gas temperature $T_g(r)$, which controls the density through the uniform pressure assumption, remains the same as above, but the electron temperature $T_e(r)$ is nearly uniform throughout the arc. The two temperature profiles are shown in Fig.9(a), along with the calculated populations of the atomic constituents in the arc from the model (b), and the comparison between the predicted H_α/H_β emission ratio and the data (c). Note that the peak electron density is 1×10^{14} cm^{-3}, which is similar to the LTE peak value of Fig.5(b). The match to the hydrogen line ratio is quite good for this model and indicates that there is a significant departure from thermal ($T_g \neq T_e$) as well as from excitation equilibrium (non-Boltzmann) in the arc mantle. The points labeled "model" in Fig.7 for the nitrogen ratios are based on the present CRE calculations.

To further investigate the plasma arc conditions a high resolution 2 meter monochrometer was fielded to measure Stark broadening of the H_β line. This broadening is related to the electron density in the line forming region. Fig.10 displays the measured H_β profile for the operating conditions of 300 Amps, 333 Volts, 90 slpm of N_2, and 4.5 slpm of H_2. The data is taken on the

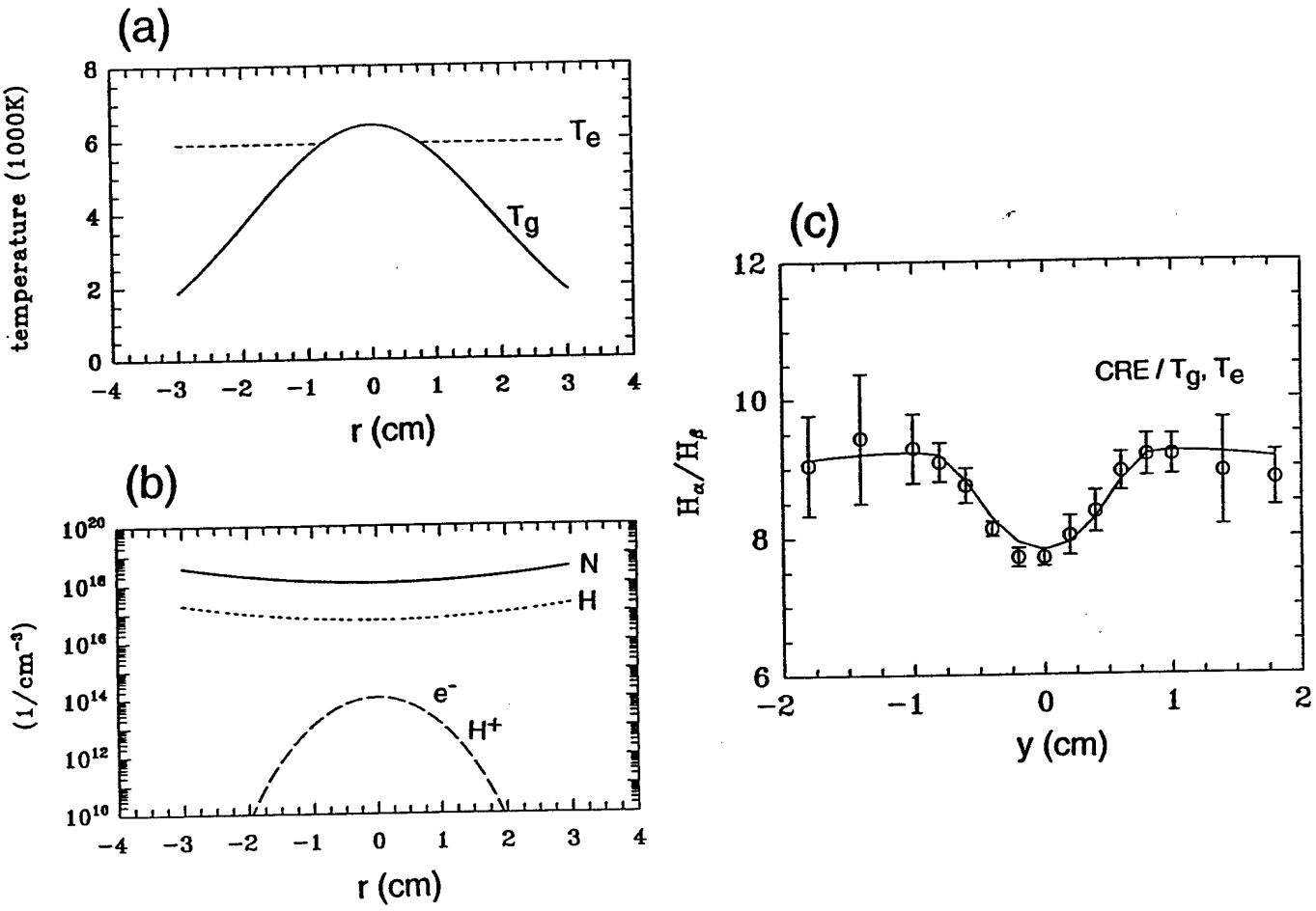

Fig.9 (a) The assumed gas T_g and electron T_e temperature profiles used for the two temperature CRE model. (b) The calculated densities of the atomic arc constituents from the model. (c) The resulting H_α/H_β emission ratio from the synthetic spectra from the two temperature model.

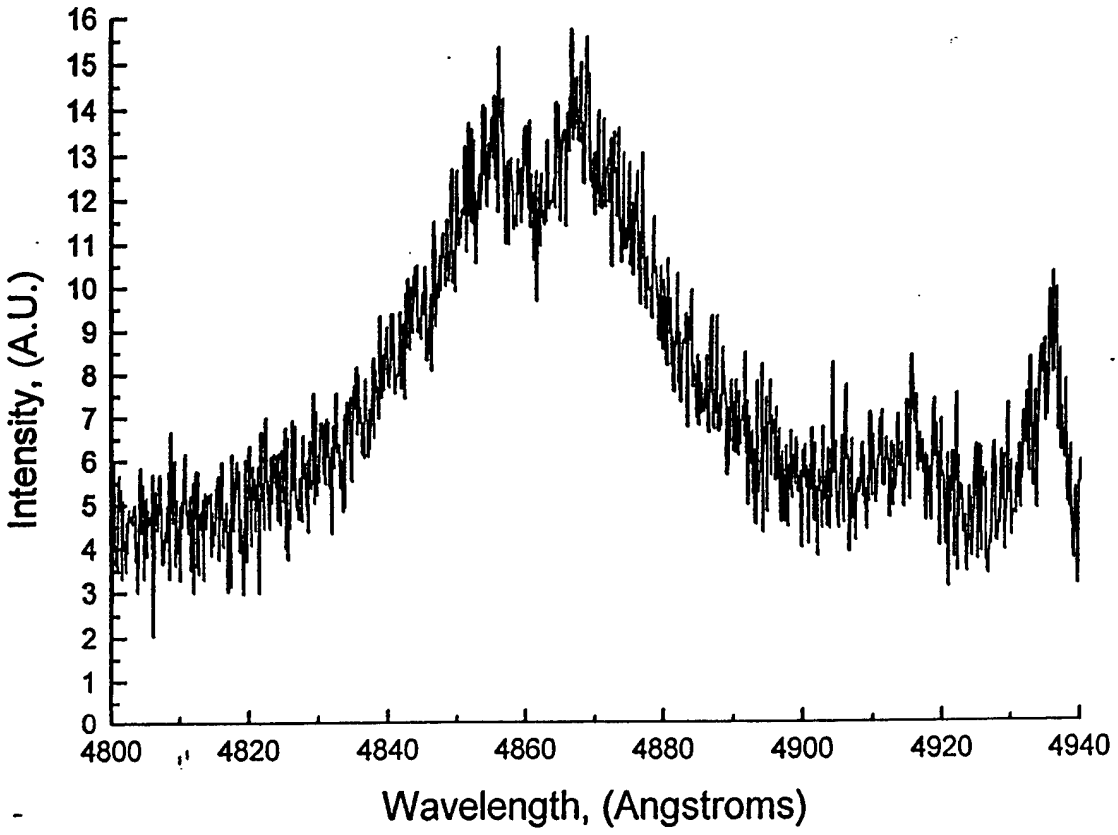

Fig.10 Measured Stark broadened profile for the H_β line at 300 Amps and 333 Volts in the non-tranferred mode. The data is taken on the arc centerline, 2 cm below the torch nozzle.

arc centerline, 2 cm below the torch nozzle. The instrumental broadening was checked with a hydrogen lamp to be only ~3 Angstroms. Using standard Stark broadened profiles for the analysis [16] and assuming a uniform plasma, the data, which presents a 38 Angstroms FWHM, indicates an electron density of 8×10^{16} cm^{-}3. This is a surprising 800 times larger than the electron density of Fig.9(c) calculated with the best fit two-temperature CRE model. The interpreted high electron density is likely to be somewhat of an overestimate since the presence of known gradients in the plasma can effect the emergent profile from which the density is inferred. A proper analysis would involve creating a synthetic profile based on the multi-frequency transport for a Stark broadened line. This calculation is more complex than the transport method used in the above CRE model which assumed a simpler Voigt emission profile.

Chen, et al., [12] used hydrogen Stark broadening to measure electron densities in a non-transferred Argon-Helium-Hydrogen arc jet. Their temperature profile was determined from absolute intensity measurements of an Argon emission line and the neighboring continuum. The densities inferred from Stark broadening, both in the arc mantle as well as downstream of the nozzle exit, were found to be several times larger than the corresponding LTE electron densities based on the measured temperature profile. The Stark broadened profiles were analyzed in the same manner as discussed above without performing a detailed radiation transfer calculation for the broadened line in the presence of plasma gradients. Chen, et al., suggest that the excess n_e is due to a population of high energy electrons (a few eV) diffusing out from the hot core of the arc near the nozzle exit orifice. Departures from equilibrium have also been observed in a transferred free burning, atmospheric pressure, arc plasma. Cram, et al., [17] computed excited level populations using the LTE assumption with a model temperature profile against the populations from a CRE model for a pure Argon arc. The results were compared with spectroscopic observations of the 4p excited state. They found that the observed density of the 4p level in the mantle of the arc is twelve orders of magnitude larger than the LTE predictions, and even two orders of magnitude above their CRE results. At the same time, Rayleigh scattering measurements of the total number density of

Argon atoms agreed with the LTE estimates. They interpreted their result of excess excited state argon as due to the absorption in the arc periphery of resonant UV radiation from the arc core.

III. OES Analysis of the Transferred Arc

Spectroscopic analysis has been also performed on the NRL torch in the transferred mode. The conditions are: 300 Volts, 330 Amps, 90 slpm of N_2, and 4.1 slpm of H_2. The spectroscopic set-up is the same as described above. The additional parameter for transferred arcs is the height above the bottom of the crucible, which is the cathode in the reverse polarity configuration of the Retech torch at NRL. Spectra were taken at various heights ranging from 10 to 26 cm. We present the analysis for the 15 cm torch height. The analysis follows the same procedure as described for the non-transferred arcs. Fig.11(a) presents five temperature profiles assumed for the plasma in the arc. A single temperature CRE model is used to calculate the excited state populations. For each of the five population distributions the H_α/H_β ratio is determined by performing the radiation transport as indicated in Fig.6(b). The resulting ratios are presented in Fig.11(b). All of the temperature profiles which decrease monotonically away from the arc center lead to values for H_α/H_β ratio that far exceed the the outermost data value at 5.5 cm y-position. Profile E is the best fit to all the data points, and as with the non-transferred data, the model suggests that the mantle of the arc is maintained through non-equilibrium processes at an elevated temperature. The central temperature determined for the transferred arc, vis., 15,000°K, is almost three times higher than found for the non-transferred arc.

Fig.12 displays the calculated atomic synthetic spectrum over the UV-vis-IR range for the transferred arc plasma corresponding to the conditions in the previous paragraph. The H_α and H_β emission lines are marked for orientation of the reader. Note the significant UV emission arising from the resonance lines of atomic nitrogen and the Lyman series of hydrogen. Integrating over the wavelength we find that the total radiated power per centimeter of arc length is $\sim$3.5 kW/cm.

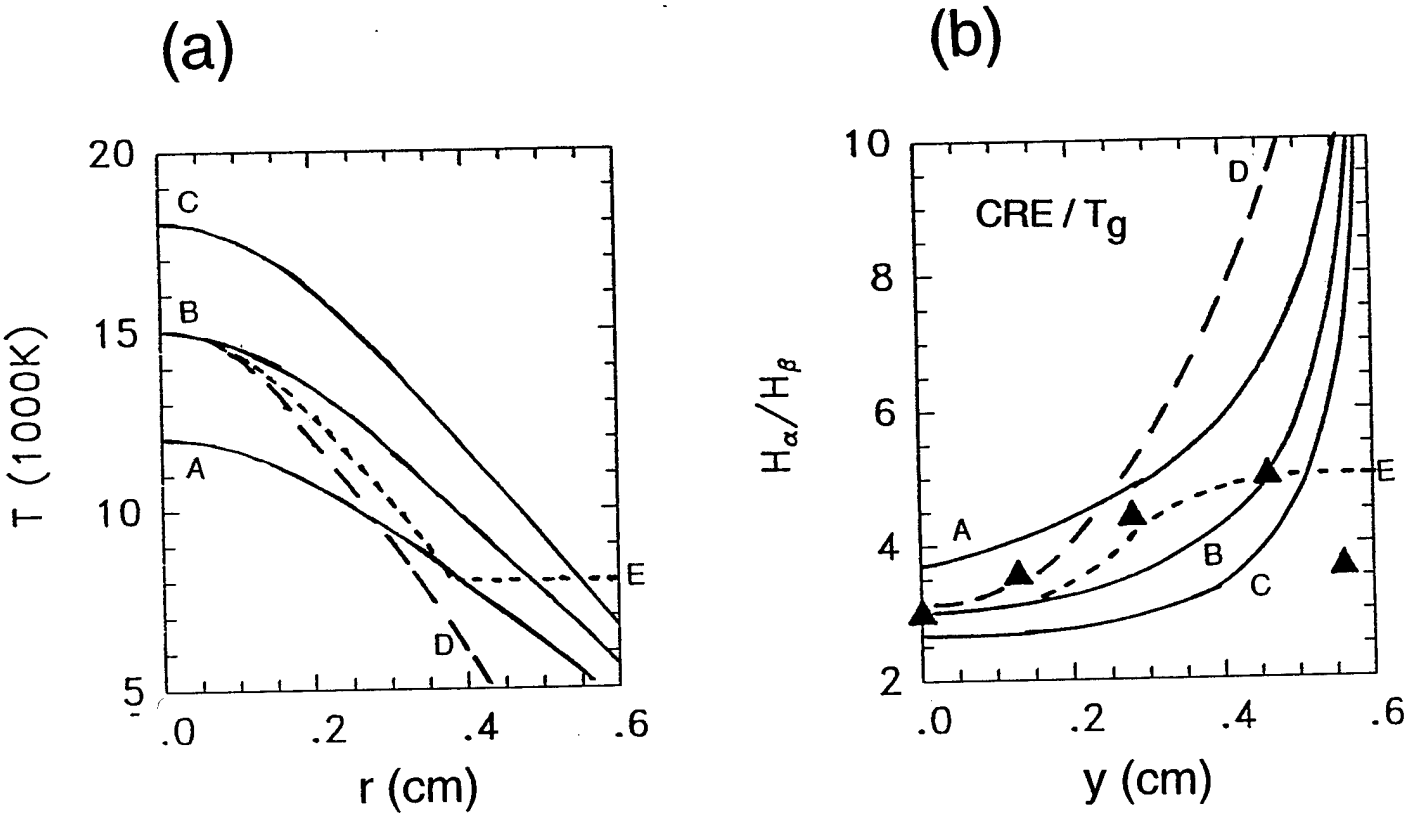

Fig.11 (a) Various temperature profiles assumed for the plasma arc in transferred mode. (b) The predicted H_α/H_β ratios from the CRE model for each of the assumed temperature profiles. Data are denoted by the solid triangles. Profile E is the best fit giving an arc core temperature of 15,000°K. Torch conditions are 300 Volts and 330 Amps, 90 slpm of N_2, 4.1 slpm of H_2, and a torch height of 15 cm above the bottom of the crucible.

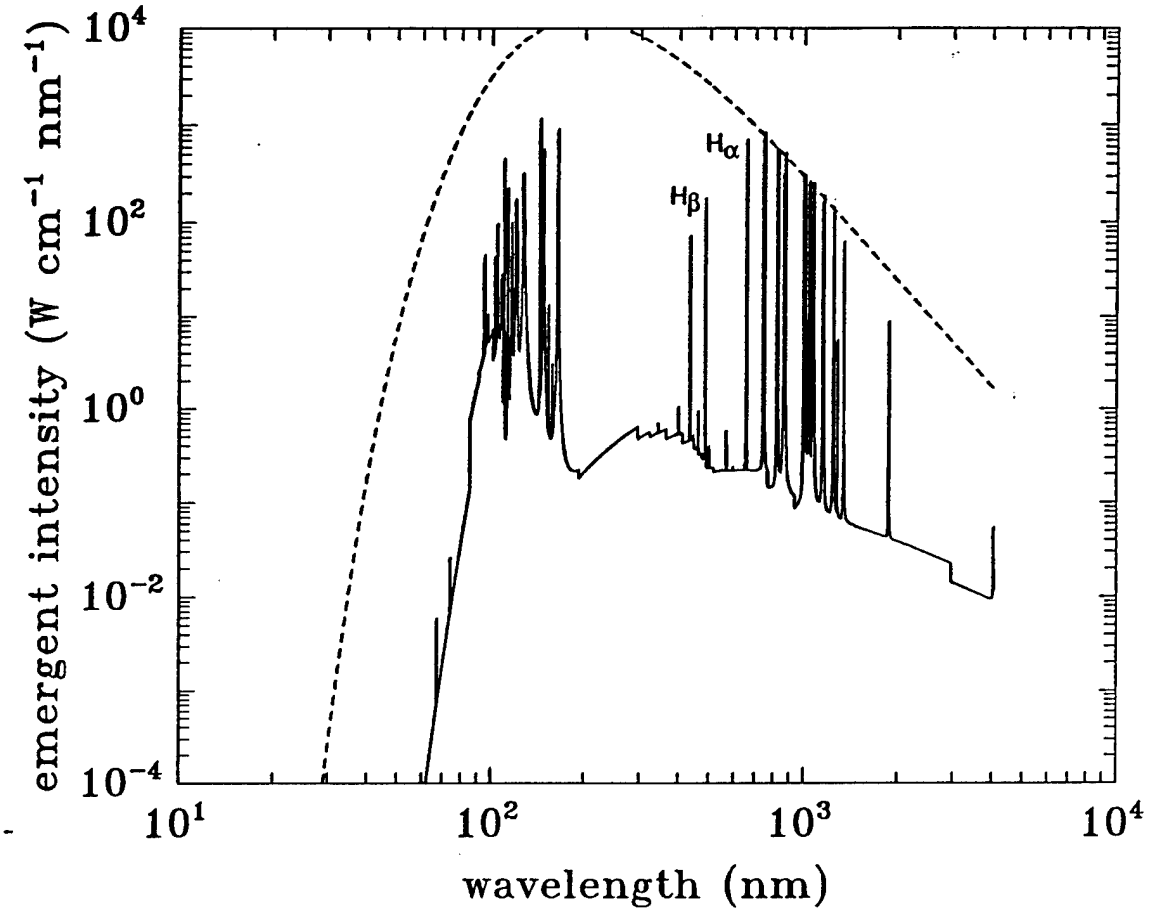

Fig.12 Synthetic emergent spectrum over the entire UV-vis-IR range based on the CRE calculations for the conditions stated in the text. The Planck spectrum at the central temperature of 15,000°K is shown as a dotted line. The effective gray body emissivity is 3.8×10^{-4}.

Given that the torch height is 15 cm, the total radiated power comprises 53% of the input power, 99 kW. For comparison the Planck emission from a 15,000°K blackbody of 1 cm diameter is shown as the dotted line. Note that the emission lines around 1000 nm are very optically thick, as they touch the blackbody limit, however, the energetic part of the spectrum is far below a blackbody emitter. The effective gray body emissivity for this plasma is estimated to 3.8×10^{-4} from the ratio of the calculated radiated power to that from the blackbody at the central temperature.

The transferred arc mode is typically used in Retech PACT systems for vitrification of solid wastes. Similar experiments were performed with the NRL torch system using a nominal waste slag consisting of iron, sand, soda glass, aluminum, titanium-oxide, aluminum silicate di-hydride, calcium carbonate, and calcium phosphate. An analysis of some of these runs revealed an interesting change in the electrical characteristics of the arc in conjunction with material entrainment from the slag vapor. Fig.13 presents data for the arc voltage as a function of height for two experiments, one using air as the working gas, the other nitrogen. For each experiment the voltage data was taken early in the run at about 15 minutes, and once more at about two hours. The electric field $\mathcal{E}$ in the arc is $d\mathcal{V}/dz$, where $\mathcal{V}$ is the measured voltage and z is the distance along the arc. Note that for both working gases $\mathcal{E}$ decreases in time for long arcs as the slag is vitrified, but remains constant for the shorter arcs. The explanation for this is found in the spectroscopic survey data. Fig.14(a) shows the spectra for a long arc (24.8 cm) observed through the centerline 3 cm below the torch nozzle and taken two hours into the slag vitrification. The strong sodium D-lines at 589.0 and 589.6 nm are shown as a single feature due to the low resolution. The sodium arises from the soda glass in the slag and is easily transformed into the vapor phase (boiling point of 1156°K at one atmosphere). The presence of the neutral sodium emission in the spectra of the long arc indicates that sodium is mixing into the arc. Since sodium has a low ionization potential (5.1 eV), it will readily ionize in the arc and enhance the free electron density in the plasma. This in turn raises the electrical conductivity of the plasma, σ, which is proportional to n_e. According to Ohm's law, the current density in the arc $\mathcal{J}$ is related to the electric field through $\mathcal{J} = \sigma\mathcal{E}$. For a constant arc

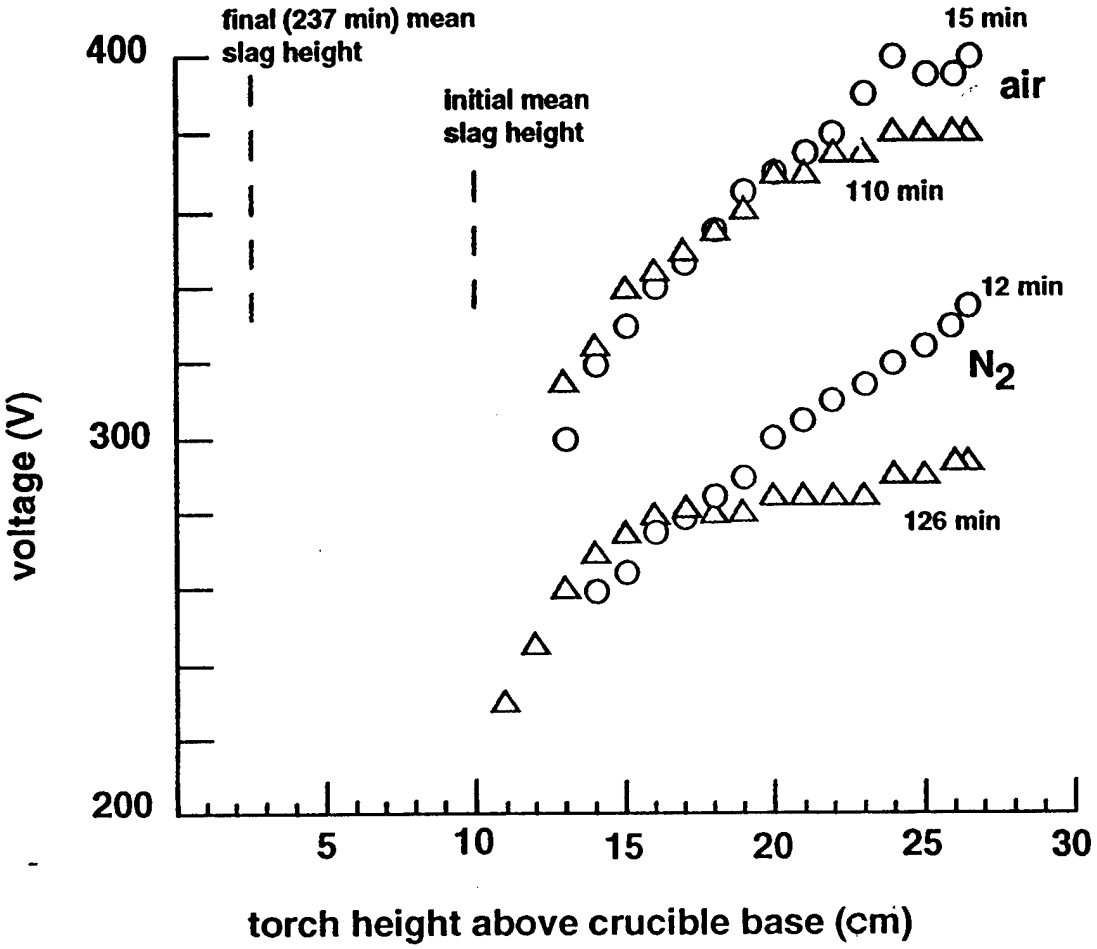

Fig.13 Voltage data for the transferred arc mode as a function of height for two experiments with different working gases. For each experiment the data was taken both early and late in the run. A change in the electrical characteristics of the arc (volts/cm) during the run is clearly seen.

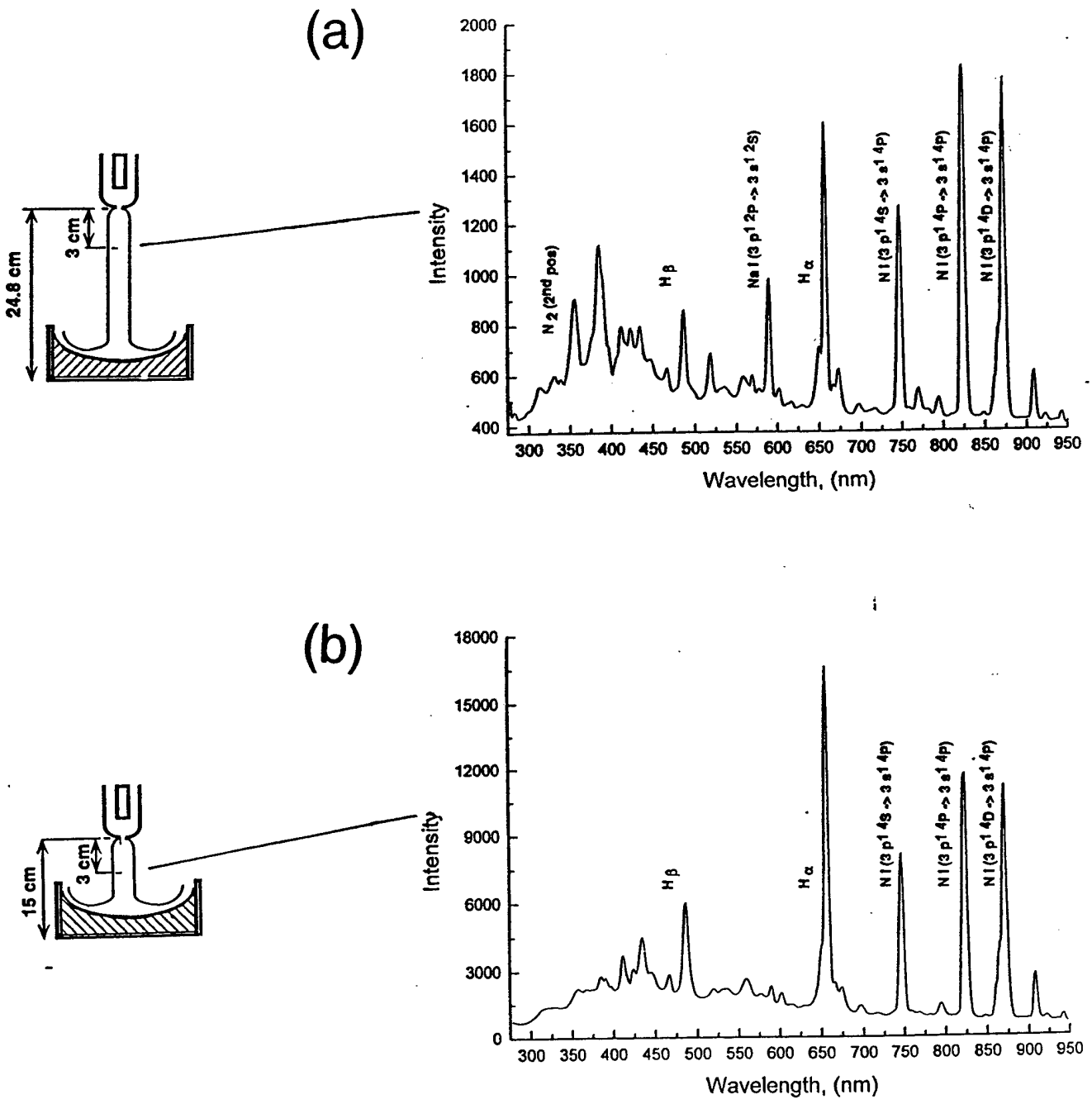

Fig.14 (a) Spectra obtained through the center of a long arc after two hours of nominal slag vitrification. (b) Similar spectra except for a short arc. The strong Na D-line emission is present in the long arc but not in the short one, indicating vapor entrainment in the former.

current and diameter, an increase in σ during vitrification due to sodium entrainment, leads to a decrease in the electric field as shown by the voltage vs height data in Fig.13. However, for short arcs, say less than 15 cm, sodium does not appear to be entrained into the arc according to the spectra in Fig.14(b). This implies that the electrical conductivity does not increase with time and the electric field remains constant, as indicated by the constancy of $\mathcal{V}$ vs z in Fig.13 for $z \leq 15$ cm.

IV. Summary

Optical spectroscopy was performed on both the non-transferred and transferred arc configurations of the NRL plasma torch. The data, in the form of emission line ratios, was analyzed using two different plasma models: LTE and CRE. The latter accounts for such processes as photo-excitation/ionization, and radiative decay/recombination. It was found that the core of the arc several centimeters below the torch nozzle exit is close to LTE, with a central temperature of 6,200°K for the non-transferred and ~15,000°K for transferred arc. For both arcs, however, the data indicate that the periphery of the arc is far from thermal and excitation equilibrium. The CRE model with the photo-processes was able to match the data if a high temperature plateau was assumed for the periphery.

Initial measurements of the Stark broadened H_β line in the non-transferred arc imply an electron density ~800 times larger than the best fit model predicts. This discrepancy needs further research, but possibly suggests that electrons from the hotter plasma formed near the cathode inside the torch body are diffusing out into the plasma jet.

For transferred arcs, the models predicts for the power balance that ~50% of the power input appears as plasma radiation. This is consistent with calorimetry measurements of the chamber cooling water which imply that 45% of the power input to the torch is absorbed by the chamber walls without slag and 65% with slag. The increase in the latter case results from re-emission by the hot slag surface. The effective gray body emissivity for the transferred nitrogen arc with

a 5% hydrogen admixture is $\sim 3.8 \times 10^{-4}$. The electrical characteristics of the transferred arc were found to change in time as a slag load was processed. Based on spectroscopic studies, easily volatized material with low ionization potentials become entrained in the arc and raise the electrical conductivity of the plasma. We suggest that this phenomena, which is readily detected by a drop in the voltage of long arcs, could be used as a diagnostic of the processed state of the slag.

Finally, we note that a plasma arc torch is more than just a heat source in waste treatment, which after all could be accomplished with standard combustion. The presence of free electrons and non-equilibrium conditions in the arc region alters the chemistry in the chamber and can enhance the breakdown of ambient or vaporized gases. The subsequent products at the freeze out temperature in exhaust line is sensitive to the arc temperature and electron density. This suggests the potential for control of the exhaust composition beyond conventional combustion and a consequent minimization of the design requirements on a secondary combustion chamber.

Acknowledgments

This work was supported by the Office of Naval Research and the Naval Surface Weapons Center, Carderock Division.

References

[1] H.W. Leutner and C.S. Stokes, "Producing Acetylene in a Plasma Jet", *Industrial and Engineering Chemistry*, Vol.**53**, pp.341-342, 1961.

[2] H. Fujimoto, H. Tokunaga and H. Iritani, "A High-Powered AC Plasma Torch for the Arc Heating of Molten Steel in a Tundish", *Plasma Chemistry and Plasma Processing*, Vol.**14**, pp.361-381, 1994.

[3] H. Herman, "Plasma-sprayed Coatings", in *Scientific American*, pp.112-117, Sept., 1988.

[4] S. Paik, G. Hawkes and H.D. Nguyen, "Effect of Working Gases on Thermal Plasma Waste Treatment", *Plasma Chemistry and Plasma Processing*, Vol.**15**, pp.677-692, 1995.

[5] S. Paik and H.D. Nguyen, "Numerical Modeling of Multiphase Plasma/Soil Flow and Heat Transfer in an Electric Arc Furnace", *International Journal of Heat and Mass Transfer*, Vol.**38**, pp.1161-1171, 1995.

[6] J.J. Gonzalez, A. Gleizes, S. Vacquie and P. Brunelot, "Modeling of the Cathode Jet of a High-Power Transferred Arc", *Plasma Chemistry and Plasma Processing*, Vol.**13**, pp.237-271, 1993.

[7] M. Cao, P. Prouix, M.I. Boulos and J. Mostaghimi, "Mathematical Modeling of High-Power Transferred Arcs", *Journal of Applied Physics*, Vol.**76**, pp.7757-7767, 1994.

[8] A. Bokhari and M. Boulos, "Energy Balance for a DC Plasma Torch", *Canadian Journal of Chemical Engineering*, Vol.**58**, pp.171-176, 1980.

[9] P.J. Parisi and W.H. Gauvin, "Heat Transfer from a Transferred-Arc Plasma to a Cylindrical Enclosure", *Plasma Chemistry and Plasma Processing*, Vol.**11**, pp.57-79, 1991.

[10] H. Maecker, "Theory of Thermal Plasma and Application to Observed Phenomena", in *Discharge and Plasma Physics*, pp.245-265, ed. S.C. Haydon, (Univ. of New England:Armidale), 1964.

[11] H. Maecker, "Arc Measurements and Results", in *Discharge and Plasma Physics*, pp.266-288, ed. S.C. Haydon, (Univ. of New England:Armidale), 1964.

[12] W.L.T. Chen, J. Heberlein and E. Pfender, "Diagnostics of a Thermal Plasma Jet by Optical Emission Spectroscopy and Enthalpy Probe Measurements", *Plasma Chemistry and Plasma Processing*, Vol.**14**, pp.317-332, 1994.

[13] D. Duston, R.W. Clark, J. Davis and J.P. Apruzese, "Radiation Energetics of a Laser-Produced Plasma", *Physical Review, A*, Vol.**27**, pp.1441-1460, 1983.

[14] J.P. Apruzese, J. Davis, D. Duston and R.W. Clark, "Influence of Lyman-series Fine-Structure Opacity on the K-Shell Spectrum and Level Populations of Low-to-Medium-Z Plasmas", *Physical Review, A*, Vol.**29**, pp.246-253, 1984.

[15] R.W. Clark, J. Davis, J.P. Apruzese and J.L. Giuliani, "A Probabilistic Model for Continuum Transport in Dense, Optically Thick Plasma", *Journal of Quantitative Spectroscopy and Radiative Transfer*, Vol.**53**, pp.307-302, 1995.

[16] H. R. Griem, *Plasma Spectroscopy*, (McGraw-Hill: New York), 1964.

[17] L.E. Cram, L. Poladian and G. Roumeliotis, "Departures from Equilibrium in a Free-Burning Argon Arc", *Journal of Physics D: Applied Physics*, Vol.**21**, pp.418-425, 1988.